

Particle size characterization and emission rates during indoor activities in a house

Tareq Hussein^{a,b,*}, Thodoros Glytsos^c, Jakub Ondráček^{c,d}, Pavla Dohányosová^d,
Vladimír Ždímal^d, Kaarle Hämeri^{a,e}, Mihalis Lazaridis^c,
Jiří Smolík^d, Markku Kulmala^a

^aDepartment of Physical Sciences, University of Helsinki, P.O. Box 64, FIN-00014 Helsinki, Finland

^bInstitute of Applied Environmental Science, Stockholm University, Frescativägen 54a, SE-10691 Stockholm, Sweden

^cDepartment of Environmental Engineering, Technical University of Crete, Polytechniopolis, GR0-73100 Chania, Greece

^dLaboratory of Aerosol Chemistry and Physics, Institute of Chemical Process Fundamentals, Rozvojová 135, CZ-16502 Praha 6, Prague, Czech Republic

^eFinnish Institute of Occupational Health, Topeliuksenkatu 41a A, FIN-00250 Helsinki, Finland

Received 25 January 2006; received in revised form 29 March 2006; accepted 31 March 2006

Abstract

Characterization and emission rates of indoor aerosols have been of great interest. However, few studies have presented quantitative determinations of aerosol particle emissions during indoor activities. In the current study we presented and investigated the physical characteristics and size-fractionated emission rates of indoor aerosol particles during different activities in a house (naturally ventilated) located in Prague, Czech Republic. We utilized a multi-compartment and size-resolved indoor aerosol model (MC-SIAM) to investigate the indoor-to-outdoor relationship of aerosol particles and also to estimate their emission rates. When the windows and the main door were closed for several hours and there were minor indoor activities that did not produce significant amounts of aerosol particles, the particle number concentration showed similar levels at different indoor locations. As expected, the natural ventilation did not provide a controlled indoor-to-outdoor relationship of aerosol particles. As previous studies have emphasized, cooking and tobacco smoking activities are major sources indoors; the total particle number concentration was, respectively, as high as 1.8×10^5 and $3.6 \times 10^4 \text{ cm}^{-3}$ with emission rates around 380 and $36 \text{ cm}^{-3} \text{ s}^{-1}$. During intensive cooking activities the outdoor aerosol particle concentrations were also affected even though windows were closed. It seems that a simple model is not able to describe the fate of indoor aerosols within a multi-compartment construction; instead, a numerical and dynamic model with a multi-compartment approach is needed. Based on the indoor aerosol model simulations, the deposition rate was comparable to previous studies with friction velocity between $10\text{--}30 \text{ cm s}^{-1}$ and surface area to volume ratio around $2.9\text{--}3.1 \text{ m}^{-1}$. The penetration factor was equivalent to G3 filter standards and the ventilation rate varied between $0.6\text{--}1.2 \text{ h}^{-1}$. Based on the emission rate analysis, aerosol particles produced during tobacco smoking and incense stick burning remain airborne for a longer time than cooking particles. It seems that aerosol particles emitted during tobacco smoking and incense stick

*Corresponding author. Department of Physical Sciences, University of Helsinki, P.O. Box 64, FIN-00014 Helsinki, Finland.
Tel.: +358 9 191 50709; fax: +358 9 191 50717.

E-mail address: tareq.hussein@helsinki.fi (T. Hussein).

burning undergo different processes; therefore, there is a need for a combined physical–chemical indoor aerosol model to better describe the evolution of indoor aerosol particles due to different activities.

© 2006 Elsevier Ltd. All rights reserved.

Keywords: Particle number size distribution; Penetration; Deposition; Natural ventilation; Modeling; Indoor sources

1. Introduction

A number of studies indicated particular correlation between deteriorated air quality and rise in asthma and respiratory allergy (e.g. Jones, 1999; Pope and Dockery, 1999; Bagley et al. 1996; Randerath et al., 1995). The public concern continues to perceive risks from poor outdoor air quality as more serious than those from indoor air (LHEA, 1997) even though numerous studies have shown that indoor concentrations of many pollutants are often higher than those typically encountered outdoors (e.g. Jones, 1999). Furthermore, people usually spend most of their time indoors (e.g. Kousa et al., 2002; Robinson and Nelson, 1995).

Indoor aerosol particles originate from both indoor and outdoor sources (e.g. Jones, 1999; Raunemaa et al., 1989). In the absence of indoor sources of aerosol particles the indoor particle concentrations show similar temporal behavior as those observed outdoors whereas during indoor activities that temporal behavior is no longer related to those outdoors; instead they are influenced with the type and strength of indoor sources. In other words, during indoor sources of aerosol particles it is no longer possible to estimate the indoor particle concentrations from those outdoors.

In general, indoor sources of aerosol particles are commonly classified according to the activities of building occupants. For example, walking generates substantial amounts of aerosol particles larger than $1\text{ }\mu\text{m}$ that are possibly re-suspended from indoor surfaces (e.g. Luoma and Batterman, 2001; Thatcher and Layton, 1995). On the other hand, fine aerosol particles are typically generated with substantial amounts during cooking, sauna heating, and fireplace (e.g. Afshari et al., 2005; Hussein et al., 2005c; Dennekamp et al., 2001; Abt et al., 2000a,b; Flückiger et al., 2000; Wallace, 2000; Long et al., 2000; Sohn et al., 1999; Siegmann and Sattler, 1996). Tobacco smoking is another major source of fine aerosol particles (Afshari et al., 2005; Lai, 2004; Morawska et al., 2003; Miller and Nazaroff, 2001; Kleeman et al., 1999; Schauer et al., 1999; Sohn et al., 1999). It was also reported that candle

burning generates aerosol particles in the diameter range $0.03\text{--}3\text{ }\mu\text{m}$ (Fine et al., 1999; Cole 1998). Air-freshener sprays also produce aerosol particles with substantial amounts (Afshari et al., 2005). Vacuum cleaners operating with or without dust bags may also produce aerosol particles (Lioy et al., 1999; Helsper et al., 1993).

Even though previous studies have characterized and discussed the effects of indoor activities on aerosol particles; few studies have presented quantitative determination of aerosol particle emissions from indoor sources (e.g. Hussein et al., 2005d; Afshari et al., 2005; He et al., 2004; Fan and Zhang, 2001). There is usually more information available on emission characteristics such as emission factors or emission rates of outdoor particle sources than of indoor sources. However, quantification of emissions from indoor sources is very important for assessment of human exposure to harmful aerosol particles.

In the current study we investigated and analyzed an indoor–outdoor aerosol data set of particle number size distributions measured in a house. The indoor aerosol particle concentrations were measured in two rooms where different indoor activities were conducted. We aimed to quantitatively investigate and characterize indoor aerosol particles during these indoor activities. We also estimated the emission rates of indoor aerosol particles by utilizing a multi-compartment and size-resolved indoor aerosol model (MC-SIAM).

2. Experimental setup

2.1. Measurement site and ambient conditions

Indoor–outdoor measurements of aerosol particles were carried out during November 16–29, 2002 in a house located about 6 km (on a plateau about 80 m high above the downtown level) north-east the downtown of Prague city. The area itself is a suburban background with minor traffic influence. There were no major pollution sources nearby the measurement site except for the Prague International Airport “Ruzyně” that was located south-west ($\sim 9\text{ km}$) of the measurement site. There was

also a main road (~ 250 m) with an average traffic density 8600 cars per day.

Basic meteorological parameters including ambient temperature, pressure, and relative humidity were measured both indoors and outdoors. The weather conditions were calm most of the time; the average wind speed was 0.5 m s^{-1} (varied between $0\text{--}2 \text{ m s}^{-1}$) and the prevailing wind direction was mostly north-western. The average indoor and outdoor temperatures were, respectively, 25.8°C (varied between $23.9\text{--}27.4^\circ\text{C}$) and 7.5°C (varied between $4.3\text{--}11.1^\circ\text{C}$). The average relative humidity was 27.7% (varied between 24.7–33.1%) indoors and 85.9% (varied between 69.7–93.1%) outdoors.

2.2. House planner and ventilation

The apartment was on the first floor of a two floor house and it was occupied by a couple. The two floors were assumed not interacting with each other via any air exchange path because they were separate constructions, there was no HVAC system, and they did not have a common entrance. The apartment consisted of a main entrance room, a hallway corridor, a bathroom, two bedrooms, a living room, and a kitchen (Fig. 1). The room doors had a small gap (less than 0.5 cm) between the door and the ground. The bathroom door was also made of wood and it had a frame that reduced the air leak

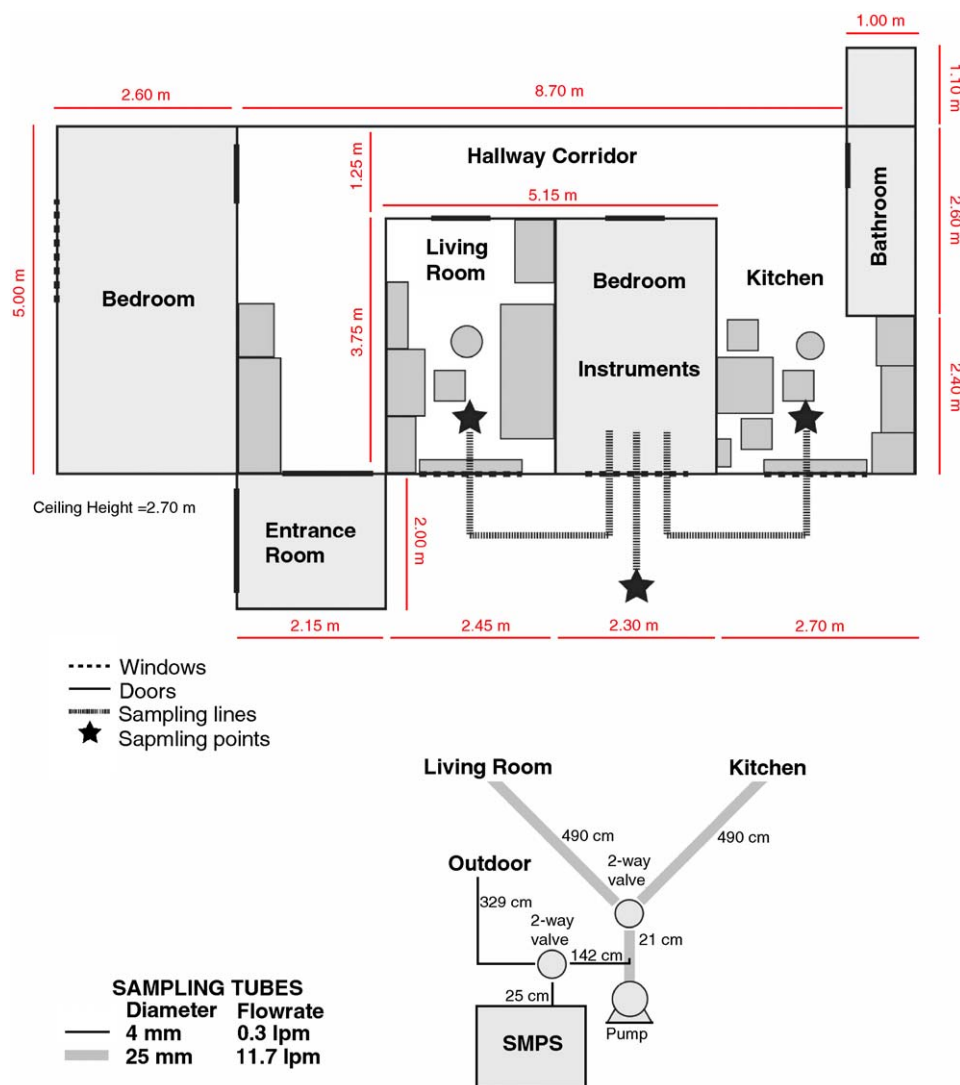


Fig. 1. A sketch showing the planner of the ground floor of the house and the measurement setup. The furniture in the kitchen and the living room is indicated with dark areas.

across the door frame. The internal door of the main entrance room was a double-wing construction. The main entrance door was double-wing construction made of metal with two glass windows and a gap (less than 0.5 cm) between the door and the ground. All internal doors except for the living room door were kept closed during the measurement period.

The house was constructed in the late sixties. The building-shell construction was made of bricks. The living room, bedrooms, and kitchen of the apartment had identical windows that were also constructed in the late sixties. The window frames were made of wood. The internal surfaces of the walls and the ceilings of the apartment were covered by plaster painted with latex. The apartment was fully furnished except for carpets. The floor material was covered by a polyvinyl-chloride (PVC) layer.

The apartment was ventilated naturally and it had a central heating; the heating radiators were located below the windows in each room. The ventilation rate was measured continuously by using constant radon supply method; in the Czech Republic, the methods using SF₆ or N₂O gases to measure the ventilation rate were not available at the time of the measurement campaign. With respect to the possible health impacts of radon gas use, the procedure was performed with very low radon concentrations below the recommended limit by the WHO organization.

The Radon gas source (emanation coefficient 0.997 and activity strength 3.6 Bq s⁻¹) was located in the room where the instrument were. We used a pump to supply a mixture of fresh air and Radon gas with a constant flow rate 12 liter per minute into the living room through plastic tubing. We used a calibrated Radon monitor (Radim3) to measure the volume activity of Radon in the living room. The measurement frequency was 30 min. This method enabled us to determine an approximate value of the ventilation rate in the living room. When the door of the living room was closed (mainly during nighttime), the mean value of the ventilation rate was $0.39 \pm 0.13 \text{ h}^{-1}$. During daytime and when the door of the living room was open, the average ventilation rate varied between $0.27\text{--}0.61 \text{ h}^{-1}$ with a mean value $\sim 0.44 \text{ h}^{-1}$.

2.3. Aerosol particle measurements

The indoor–outdoor aerosol measurements consisted of particle number size distributions (14–552 nm) with a

Scanning Mobility Particle Sizer (SMPS 3934C, TSI Inc., USA). The air sampling was performed sequentially from outdoors, kitchen, and living room by using valve selectors (Fig. 1). The valves were controlled with two programmable controllers that used the CPC voltage (controlling the high voltage on the central rod of the DMA) in the SMPS as a signal for switching. One particle number size distribution scan was performed within 5 min. In every scan, the cycle of the DMA voltage was 10–10 000 V within 3 min and then back to 10 V in the following minute; and then it was followed by 1 min waiting period to flush the sampling lines. The sequential air sampling included two scans from outdoors followed by two scans from the kitchen and then two scans from the living room during the whole measurement period except for November 22–25, 2005, when the sampling cycle was two scans outdoors followed by one scan from the kitchen and two scans from the living room and finally one scan from the kitchen. The sample flow rate into the SMPS was 0.3 l min^{-1} and the sheath flow rate was 3 l min^{-1} . The SMPS was calibrated prior to the measurement campaign according to the standard procedure recommended by the TSI Inc.

The SMPS was located in the bedroom between the kitchen and the living room (Fig. 1). The outdoor air sampling was performed at 1.5 m from the ground in front of the bedroom (between the kitchen and the living room). The indoor air samplings in the kitchen and the living room were also performed at 1.5 m from the ground. The sampling lines were led to the bedroom through the windows from every sampling location. The sampling lines were made of stainless steel. There were no special inlets or air drier installed on the sampling lines except for a rain cover for the outdoor air sampling line. The transport efficiency of the sampling lines was considered in the raw data. The raw data of the particle number size distributions were extracted from the SMPS by using the Aerosol Instrument Manager Software (version 4.3. TSI Inc., USA).

3. Data analysis and modeling

3.1. Data handling and interpretation of the particle number size distributions

The raw data of the particle number size distributions were interpolated to a common time (15 min resolution) and particle size grid (40 bins

between 15–530 nm). We interpreted the *I/O* ratios from their median and quartiles values. We also parameterized the particle number size distributions with the multi log-normal distribution function

$$\frac{dN}{d\log(D_p)} = \sum_{i=1}^n \frac{N_i}{\sqrt{2\pi} \log(\sigma_{g,i})} \times \exp\left[-\frac{(\log(D_p) - \log(\bar{D}_{pg,i}))^2}{2\log^2(\sigma_{g,i})}\right], \quad (1)$$

where D_p is the aerosol particle diameter. Three parameters characterize an individual log-normal mode i are the mode number concentration N_i , geometric variance $\sigma_{g,i}^2$, and geometric mean diameter (GMD) $\bar{D}_{pg,i}$. The number of individual log-normal modes that characterize the particle number size distribution is denoted by n . The parameterization was according to the principles described by Hussein et al. (2005a); we set the maximum number of modes to three and the algorithm was allowed to reduce that number to one without affecting the fitting quality. The multi log-normal distribution function has been commonly used to parameterize the particle number size distributions indoors and outdoors (e.g. Hussein et al., 2005a–c; Hussein et al., 2004a,b; Birmili et al., 2001; Mäkelä et al., 2000; Morawska et al., 1999; Whitby, 1978).

3.2. Indoor aerosol modeling: an aerosol dynamics model

The dynamic behavior of aerosol particles and their transport indoors can be studied with mathematical models that describe the change rate of aerosol particle concentrations. Indoor air is commonly assumed well-mixed, i.e. single-compartment approach (e.g. Smolik et al., 2005; Asmi et al., 2004; Jamriska et al., 2003; Riley et al., 2002; Thornburg et al., 2001; Mosley et al., 2001; Abt et al., 2000a,b; Thatcher et al., 2002; Jamriska et al., 1999; Kulmala et al., 1999; Thatcher and Layton, 1995; Nazaroff et al., 1993; Ott et al., 1992; Repace and Lowrey, 1980). Even though this description is appropriate to some extent (Klepeis, 1999; Ott et al., 1996) there is still a need to describe indoor environments with a multi-compartment approach when the indoor air is not well-mixed or when the indoor space consists of more than one room (e.g. Hussein et al., 2005d; Lai, 2004; Gadgil et al., 2003; Haas et al., 2002; Miller and Nazaroff, 2001; Borchellini and Fürbringer, 1999; Feustel, 1999; Schneider et al., 1998; Shimada

et al., 1996; Nazaroff and Cass, 1986, 1989); i.e. pollutant concentrations vary markedly indoors.

In the current study we utilized the MC-SIAM. The MC-SIAM algorithm is capable of simulating and investigating the indoor–outdoor relationship of aerosol particles (Hussein et al., 2005d) and the evolution of aerosol particles is based on a modified and extended dynamic scheme of the aerosol model UHMA (Korhonen et al., 2004). The deposition of aerosol particles onto available indoor surfaces is based on the model described by Lai and Nazaroff (2000). As a special feature in the MC-SIAM algorithm, it has been developed to estimate the emission rates of indoor aerosol particles during different indoor activities. The emission rate estimation is based on a semi-empirical method; the mathematical difference between measured and simulated (by ignoring indoor sources) after taking into account the effects of removal processes such as deposition, ventilation, air exchange rates, etc.

According to the MC-SIAM algorithm, the particle-size-specific balance equation of the number concentration in each compartment is described by

$$\begin{aligned} \frac{d}{dt} N_{k,D_p} = & \frac{1}{V_k} \sum_m Q_{mk} P_{m,D_p} N_{out,D_p} - \frac{1}{V_k} Q_{k,removed} N_{k,D_p} \\ & + \frac{1}{V_k} \sum_j (Q_{jk} N_{j,D_p} - Q_{kj} N_{k,D_p}) \\ & - \frac{1}{V_k} \sum_i A_{ki} v_{ki,d,D_p} N_{k,D_p} \\ & + \frac{1}{V_k} \sum_i f_{ki,D_p} A_{ki} \lambda_{ki,re,D_p} B_{ki,D_p} \\ & + J_{k,source,D_p} - J_{k,l \sin k,D_p} + J_{k,co,D_p} \\ & + J_{k,cond,D_p} + J_{k,nuc,D_p} + \sum_{other} J_{k,other,D_p}, \quad (2) \end{aligned}$$

where every term in Eq. (2) is listed and described in Table 1. Currently, the re-suspension process of aerosol particles from indoor surfaces is not yet well-understood; only few studies modeled this process (e.g. Theerachaisupakij et al., 2003; Friess and Yadigaroglu, 2002; Lazaridis and Drossinos, 1998). Because there has not been a generalized approach that can be utilized in the current version of MC-SIAM we include the re-suspension process in the emission source term.

3.3. Fate of indoor aerosols: a simplified indoor aerosol model

Under certain conditions, the indoor–outdoor aerosol problem can be simplified and the fate of

Table 1
Indoor aerosol model parameters and terms

Parameter	Units	Description
$N_{k,Dp}$	m^{-3}	Number concentration of aerosol particles in compartment k
$N_{j,Dp}$	m^{-3}	Number concentration of aerosol particles in compartment j
$N_{out,Dp}$	m^{-3}	Outdoor number concentration of aerosol particles
$S_{k,Dp}$	m^{-3}	Difference between measured and simulated aerosol particle number concentrations. Suspended emitted aerosol particles
$B_{ki,Dp}$	m^{-2}	Aerosol particle number concentration accumulated on an indoor surface i of area A_{ki}
$P_{m,Dp}$	–	Penetration factor of aerosol particles via path m
Q_{mk}	$m^3 s^{-1}$	Air flow rate that brings outdoor aerosol particles with a concentration $N_{out,Dp}$ via path way m
$Q_{k,removed}$	$m^3 s^{-1}$	Removed air flow rate from compartment k into the outdoor air
Q_{jk}	$m^3 s^{-1}$	Air flow rate from compartment j into compartment k
$v_{ki,d,Dp}$	$m s^{-1}$	Deposition velocity of aerosol particles onto indoor surfaces. This term is estimated with the model developed by Lai and Nazaroff (2000)
$f_{ki,Dp}$	–	Fraction of the accumulated aerosol particles available for re-suspension from an indoor surface with a re-suspension rate $\lambda_{ki,re,Dp}$
$\lambda_{ki,re,Dp}$	s^{-1}	Re-suspension rate of aerosol particles from an indoor surface i
A_{ki}	m^2	Total area of a deposition surface i in compartment k
V_k	m^3	Volume of compartment k
$J_{k,cond,Dp}$	$m^{-3} s^{-1}$	Condensation: an aerosol dynamic process implemented from UHMA
$J_{k,co,Dp}$	$m^{-3} s^{-1}$	Coagulation: an aerosol dynamic process implemented from UHMA
$J_{k,nuc,Dp}$	$m^{-3} s^{-1}$	Nucleation: an aerosol dynamic process implemented from UHMA
$J_{k,source,Dp}$	$m^{-3} s^{-1}$	Process: indoor source of aerosol particles. “Emission rate term”
$J_{k,sink,Dp}$	$m^{-3} s^{-1}$	Process: aerosol particles lost by indoor sinks
$J_{k,other,Dp}$	$m^{-3} s^{-1}$	Change rate of aerosol particle number concentrations due other possible processes to be considered in the indoor aerosol model

indoor aerosol particles can be estimated analytically. The use of a simplified indoor aerosol model requires the following conditions: (1) the indoor air is assumed well-mixed and there are no concentration gradients indoors, (2) the effects of coagulation, nucleation and condensation processes are negligible, and (3) the indoor compartment of interest does not interact with other indoor compartments. Otherwise, the incoming air that brings aerosol particles from other compartments can be handled within the source term and similarly the outgoing air that take out aerosol particles from that compartment of interest can be considered as removal processes.

In a simplified indoor aerosol model the balance equation is defined as follows:

$$\frac{dI_{Dp}}{dt} = \lambda \cdot P_{Dp} \cdot O_{Dp} - (\lambda + \lambda_{deposition,Dp})I_{Dp}, \quad (3)$$

where the subscript D_p indicates that the equation is valid for a certain particle size range ΔD_p . I and O are the particle number concentrations [m^{-3}] indoors and outdoors, respectively. P is the penetration factor. λ is the ventilation rate [s^{-1}]. λ_{decay} is the particle loss rate [s^{-1}] due to all other removal

processes including deposition of aerosol particles into indoor surfaces. Eq. (3) has an analytical solution if we assume that the outdoor particle number concentrations are approximately constant (e.g. Hussein et al., 2005c).

Starting an indoor source that generates aerosol particles with significantly high number concentrations within a short period of time and after that it is turned off (at time = t_0), the particle loss rate, i.e. λ_{decay} , is then described as follows:

$$\lambda_{decay,Dp} \cong \frac{1}{\Delta t} \ln \left(\frac{I_{Dp}(t_0)}{I_{Dp}(t_0 + \Delta t)} \right) - \lambda. \quad (4)$$

Note that λ_{decay} represents a combination of several removal processes including deposition on indoor surfaces.

4. Results and discussion

4.1. Indoor-to-outdoor relationship of aerosol particles

In the absence of indoor activities and when the windows and the main door were closed for a long time period (more than 5 h), the particle number

concentration in both the kitchen and the living room maintained rather similar levels of number concentrations (Fig. 2). As expected, the temporal variations of the indoor particle number concentrations were similar to that outdoors with a varying time-lag and lower concentrations. The varying time-lag was due to the natural ventilation (e.g. Hussein et al., 2005c). Under the same conditions, we expect that the number concentrations in other rooms have similar temporal variation and absolute values as that observed in the kitchen and the living room.

During the whole measurement period (no indoor activities), the median value of the total particle number concentrations (15–530 nm) was about 1800 cm^{-3} outdoors, 1600 cm^{-3} in the kitchen, and 1650 cm^{-3} in the living room (Table 2). The ultrafine particles (UFP, diameter < 100 nm) contributed more than 55% of the total particle number concentration outdoors; this is rather small value. That can be due to the fact that we measured the

size distributions based on their wet electrical-mobility diameters instead of their dry electrical-mobility diameter. The corresponding contribution of UFP in the kitchen and the living room air varied between 40–80%, which was possibly due to the

Table 2

Particle number concentrations (mean, median, standard deviation, and quartiles) evaluated for the whole measurement period (November 16–29, 2002)

		25%	Median	75%	Mean	SD
15–530 nm	Outdoor	1128	1798	4138	2947	3151
	Kitchen	963	1617	4550	5979	19 175
	Living room	951	1657	5271	4749	12 230
15–100 nm	Outdoor	576	972	2667	1721	1989
	Kitchen	463	848	2446	4135	15 828
	Living room	452	792	2621	2956	10 063
100–530 nm	Outdoor	497	809	1582	1237	1310
	Kitchen	476	733	1785	1855	5044
	Living room	476	760	2116	1805	4210

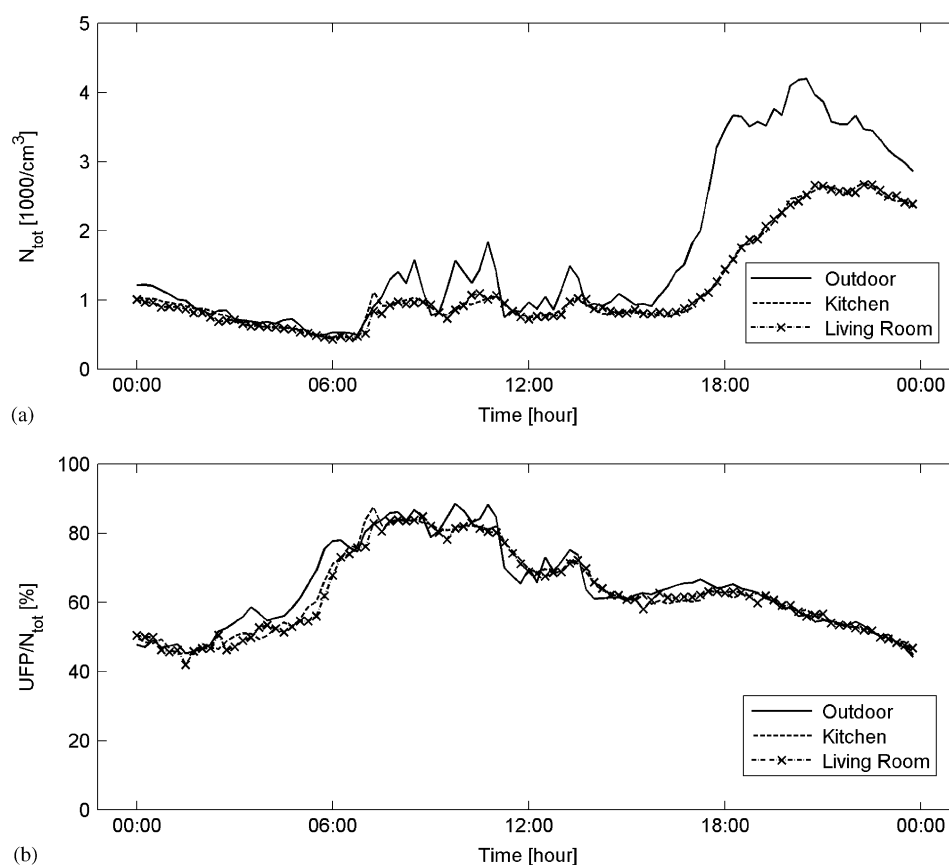


Fig. 2. An example of one day without indoor activities: (a) total particle number concentrations (15–530 nm); (b) percentage contribution of UFP (diameter < 100 nm).

varying penetration factor and air exchange rate. The building structure was also very old and it was leaking considerably even when the windows were closed. This influences the penetration factor that shows considerable dependence on the weather conditions (e.g. Chan, 2002). In general, the natural ventilation does not provide a well-controlled penetration factor and air exchange rate (e.g. Hussein et al., 2005c).

In Tables 3 and 4 are listed the modal structures of the indoor and outdoor aerosol particles. About 53% of the outdoor particle number size distributions were parameterized with three log-normal modes with GMD < 75 nm, between 75 and 175 nm, and > 175 nm (Fig. 3a). About 43% were parameterized with two log-normal with GMD < 85 and > 85 nm. By ignoring the fact that we measured particle mobility distributions without an air drier; i.e. wet diameter, this modal structure seems to be a characteristic of aerosol particles in central Europe. For example, Birmili et al. (2001) reported dry mobility distributions with 2–5 log-normal modes, and the modal structures with 2–3 log-normal modes are comparable to what we observed in the current study.

The indoor particle number size distributions (about 47% of all cases measured in the kitchen and 48% in the living room) were parameterized with

three log-normal modes (Fig. 3b,c). About 40.5% in the kitchen and 37.5% in the living room were parameterized with two log-normal modes. In these parameterizations with three and two log-normal modes, the GMD ranges were rather similar to those observed outdoors. The remaining cases (about 12.5% in the kitchen and 14% in the living room) were parameterized with a single log-normal mode that was observed during some indoor activities (such as cooking, tobacco smoking, and incense stick burning). The physical characteristics of this mode varied considerably with the varying indoor activity.

4.2. Indoor-to-outdoor concentration ratios (*I/O*)

The *I/O* values were analyzed by ignoring the time periods of indoor activities. Because of the natural ventilation, i.e. varying ventilation rate and penetration factor, we observed variable *I/O* values and time-lag between the indoor and outdoor particle number concentrations. Instead of shifting the number concentrations searching for the best correlation between the temporal variations of indoor and outdoor particle number concentrations we expressed the *I/O* values by their means, standard deviations, medians, and quartiles or percentiles. In general, when the air exchange rate

Table 3
Median values of the multi-lognormal parameters that describe the modal structure of the particle number concentrations for all cases including uni-modal, bi-modal, and tri-modal fitting

	Mode-1			Mode-2			Mode-3		
	$N_{,1}$ (cm ⁻³)	$D_{pg,1}$ (nm)	$\sigma_{g,1}$	$N_{,2}$ (cm ⁻³)	$D_{pg,2}$ (nm)	$\sigma_{g,2}$	$N_{,3}$ (cm ⁻³)	$D_{pg,3}$ (nm)	$\sigma_{g,3}$
Outdoor	663	35.3	1.75	1067	115.8	1.77	284	268.3	1.59
Kitchen	552	37.8	1.75	879	118.2	1.75	219	251.2	1.52
Living room	547	37.6	1.75	893	118.2	1.75	223	251.2	1.50

Table 4
Median values of the multi-lognormal parameters that describe the modal structure of the particle number concentrations for the uni-modal cases

	Mode-1a			Mode-1b		
	$N_{,1a}$ (cm ⁻³)	$D_{pg,1a}$ (nm)	$\sigma_{g,1a}$	$N_{,1b}$ (cm ⁻³)	$D_{pg,1b}$ (nm)	$\sigma_{g,1}$
Kitchen	33 543	73.0	1.64	1507	123.6	1.89
Living room	23 704	98.2	1.67	1554	123.6	1.87

Mode-1a represents the particle number size distributions during their formation in the indoor air. Mode-1b represents the particle number size distributions in the indoor air that originate from outdoor origin.

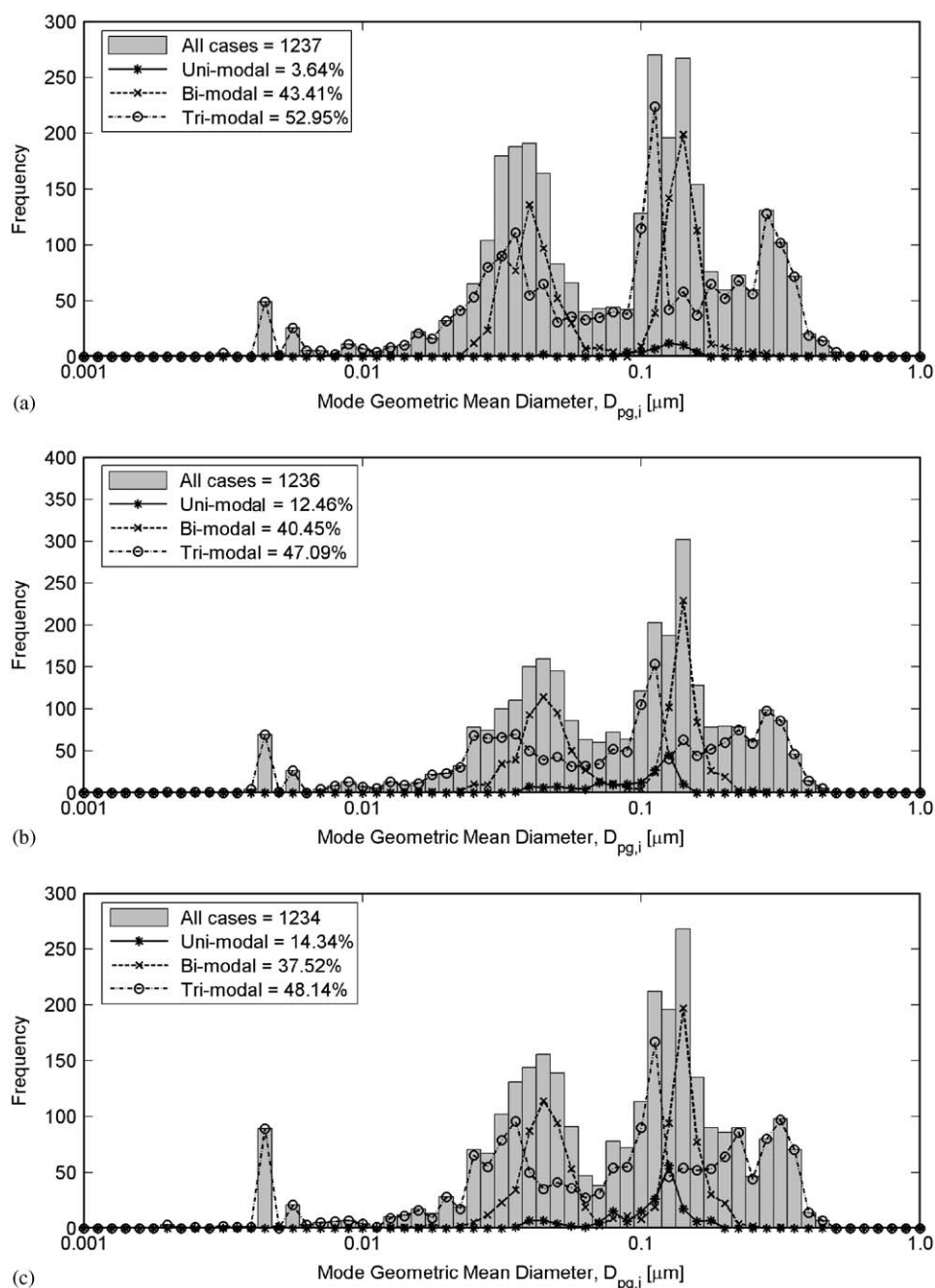


Fig. 3. Modal structure of the particle number size distribution that was extracted from the mode geometric mean diameter ($D_{pg,i}$). (a) outdoors; (b) kitchen; and (c) living room. Note that the measured particle number size distributions in the current study were based on their wet electrical-mobility diameters.

is well-controlled, the temporal variation of the indoor aerosol particle number concentrations can be shifted systemically to obtain the I/O values (e.g. Morawska et al., 2001). On the other hand, the time-lag can be neglected when the air exchange rate is rather high ($> 2 \text{ h}^{-1}$) because the indoor particle

number concentrations adjust rapidly with the varying outdoor particle number concentrations (Hussein et al., 2004a).

In general, the I/O curves for both the kitchen and the living room showed rather similar behavior (Fig. 4). Based on the median values, the I/O curves

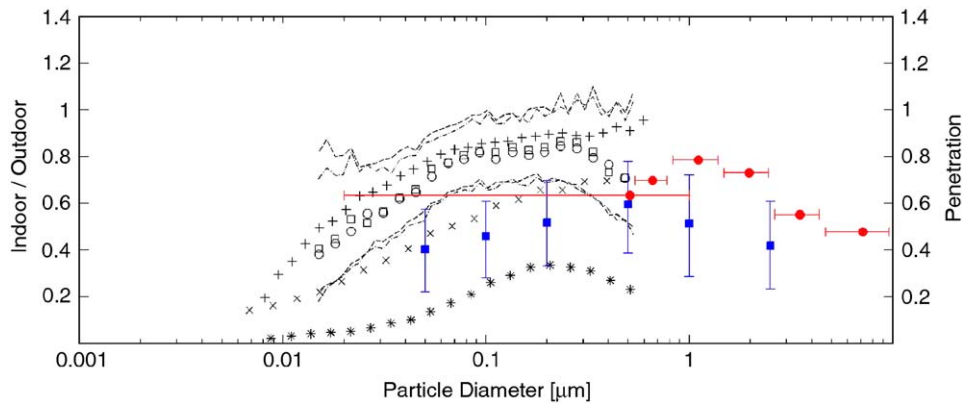


Fig. 4. Indoor-to-outdoor ratios of particle number concentrations versus particle size. The curves were evaluated as medians and quartiles for the whole measurement period and by excluding the time periods when indoor activities and their effects took place in the indoor air. All presented curves represent *I/O* ratios except for the results by Thornburg et al. (2001) that shows the penetration factor. Note that the measured particle number size distributions in the current study were based on their wet electrical-mobility diameters. Mechanical ventilation: * Koponen et al. (2001), F7-class; + Hussein et al. (2004), G3-class. Natural ventilation: × Hussein et al. (2005c); — Chao et al. (2003); ‡ Thornburg et al. (2001). Current Study: □ Kitchen; - - - - Kitchen, quartiles; ○ Living room; - - - - Living room, quartiles.

had a maximum between particle diameters 0.1–0.4 μm, which indicates maximum penetration factor within the particle diameter range 0.1–1.0 μm. This agrees with the general penetration theory (Hinds, 1999). The *I/O* ratios for UFP ranged between 0.4–0.8 and those for accumulation mode particles ranged between 0.7–0.8. The *I/O* values obtained in the current study are within a similar level of *I/O* values and penetration factor values observed in other dwellings ventilated naturally (e.g. Hussein et al., 2005c; Chao et al., 2003, Thornburg et al., 2001). On the other hand, when compared to other indoor environments with mechanical ventilation systems standard filters, the *I/O* values obtained in the current study are relatively comparable to G3 filter standards installed in an office room (Fig. 4).

4.3. Fate of indoor aerosols

Here, the fate of aerosol particles was investigated for the aerosol data measured in the kitchen only. However, in the model simulations analysis we will discuss the fate of aerosol particles in both the living room and the kitchen. We kept our analysis for cooking activities only because they produced aerosol particles within a wide particle size range and they were repeated several times that provided an overall average curve for the particle loss rate as a function of particle diameter.

According to Eq. (4), the average particle loss rate was about 4 h^{-1} for particles 0.02 μm in diameter and about 0.1 h^{-1} for 0.5 μm particles. The particle loss rate obtained in the current study is rather higher in comparison to previous studies (Fig. 5). In fact, the particle loss rate, i.e. λ_{decay} , obtained in the current study does not represent the particle deposition rate only; it also includes a combined effect of different aerosol particle removal processes due to the interaction between the kitchen and the living room. In other words, the kitchen itself is an open area to the hallway and when cooking activities took place in the kitchen while the living room door was opened, the particle number concentrations in the living room were elevated as a result of the air exchange between the kitchen and the living room. Meanwhile, the aerosol particles were re-circulated back to the kitchen (source area) after undergoing several deposition pattern and removal processes in the living room. This would indeed affect our results for estimating the particle loss rate in the kitchen.

The deposition rate for each particle size on indoor surfaces can be estimated according to

$$\lambda_{\text{deposition}, D_p} = \sum_{j=\text{surfaces}} \frac{A_j}{V} v_{d, D_p j}, \quad (5)$$

where j runs over all possible surfaces of deposition, $A_j [\text{m}^2]$ is the total surface area of a deposition

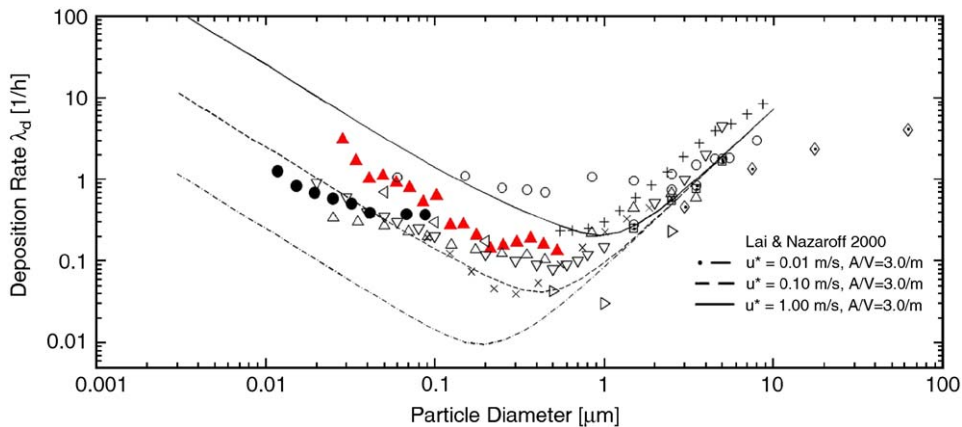


Fig. 5. Particle loss rates obtained in the current study (filled triangles) and compared to previous studies. The lines represent calculated deposition rates using the model of Lai and Nazaroff (2000) for deposition velocity; the input parameters of the model: A/V is the total indoor surface area to the total room volume ratio and the friction velocity (u^*). Note that the measured particle number size distributions in the current study were based on their wet electrical-mobility diameters. \times : Offermann et al. (1985); ∇ : Mosley et al. (2001); \triangle : Long et al. (2001); \square : Thatcher & Layton 1995 ($\lambda = 0.30/h$); \odot : Thatcher & Layton (1995) ($\lambda = 0.18/h$); \diamond : Thatcher & Layton (1995) ($\lambda = 0.14/h$); \triangleleft : Thornburg et al. (2001) ($A/V = 0.333/m$); \triangleright : Thornburg et al. (2001) ($A/V = 1.750/m$); $+$: Thatcher et al. (2002). \bullet : Hussein et al. (2005c); \blacktriangle : This Study; \circ : Abt et al. (2000b).

Table 5

Net indoor surface area (m^2) and volume (m^3); the furniture was included

	Surface area			Volume
	Upward	Downward	Vertical	
Entrance hall	11.14	11.14	35.24	27.42
Living room	11.18	11.18	51.74	22.63
Kitchen	15.99	15.99	44.56	28.39

surface j , $V [m^3]$ is the net volume of the room, and $v_{d,D_{p,j}} [ms^{-1}]$ is the aerosol particle deposition velocity on that surface. The deposition velocity can be obtained by using a model developed by Lai and Nazaroff (2000) that requires the friction velocity and particle size as input parameters.

In our analysis, we used the net indoor surface area and volume of the living room (Table 5). According to this model study by Lai and Nazaroff (2000), the friction velocity that represents the obtained particle loss rate would be $0.1\text{--}1.0\text{ ms}^{-1}$ when the mean surface area-to-volume ratio is $2.9\text{--}3.1\text{ m}^{-1}$. As will be shown from the indoor aerosol model simulations later in this study, this friction velocity is rather high for the same reason mentioned before in this section and also because of unknown processes not considered in the analysis and model simulations.

4.4. Indoor activities

The residents reported the type, time period, and location of the indoor activity. They also reported the time periods when the living room door and window were opened. The residents did not follow a certain daily pattern for their activities; however, they used to get up in the morning between 06:00 and 07:00 and they used to go to bed around midnight. Cooking activities included frying and use of oven and stove in the kitchen. All other activities (candles, aroma lamp, incense stick, tobacco smoking, hair drier, and hair spray) took place in the living room. The residents used the bathroom and they used to sleep in the bedroom. The doors of all other rooms including the bathroom and the bedroom were kept closed most of the time except for very short periods that can be neglected from the data analysis.

As previous studies reported, major sources of indoor aerosol particles are cooking and tobacco smoking. In the current study we report that incense stick can be also considered an intermediate source of indoor aerosol particles. However, candle burning and aroma lamp were less significant sources indoors in comparison with cooking and tobacco smoke. In some occasions cooking and other activities occurred at the same time, therefore, the effect of other activities was not observable because cooking activities is a stronger source.

Consequently, we skipped these occasions from the analysis and model simulations.

4.4.1. Cooking

Cooking activities were performed on an electrical stove and they included some of the following: boiling potatoes, soup, rice, pasta, frying (potatoes or pancakes), toasting, and baking chicken (in oven). In some occasions, the food was only warmed up.

Cooking activities produced aerosol particles with total number concentrations exceeding $1.8 \times 10^6 \text{ cm}^{-3}$ (more than 90% is UFP) in the kitchen (Fig. 6). The effect was observed within the whole measured size range (Fig. 7a). The life-time of the cooking aerosol particles in the kitchen varied between 4–6 h. The particle number concentrations in the living room were also affected significantly when the living room door was opened. The total particle number concentration in the living room was at least 0.3 its value in the kitchen with a time-lag varied between few minutes to half an hour (Fig. 6). Even when the living room door was closed, the particle number concentrations in the living room showed a slight increase during cooking activities; peak value in the living room was about 0.1 its value in the kitchen (Fig. 6d). The varying time-lag is apparently related to the varying air exchange rate between the kitchen and the living room.

It was previously reported that the maximum total particle number concentration of fine and coarse particles vary between 1.5×10^6 and $5.6 \times 10^6 \text{ cm}^{-3}$ during different kinds of cooking activities (e.g. Afshari et al., 2005; Hussein et al., 2005c; He et al., 2004; Morawska et al., 2003; Dennekamp et al., 2001; Abt et al., 2000a; Siegmann and Sattler, 1996). Apparently, the wide variation in the particle number concentration during cooking activities is related to the type of cooking as well as the building conditions including geometry, ventilation, and stove location with respect to the measurement point. For example, cooking on a gas stove seems to produce more particles than cooking on an electrical stove; the maximum value was around $1.1 \times 10^6 \text{ cm}^{-3}$ when cooking on an electrical stove whereas it was as high as 5.6×10^6 when cooking on a gas stove (Dennekamp et al., 2001).

4.4.2. Candle burning

Burning candles occurred only once in the living room; we observed a slight increase in the total

number concentrations of particles $<0.02 \mu\text{m}$ in diameter (Figs. 6a and 7b). After extinguishing the candle burning, the number concentrations of particles $<0.03 \mu\text{m}$ in diameter showed significant increase (2000 cm^{-3} over the base-line) in the living room (Fig. 7b). It was also shown that extinguishing candles produces more particles than during the burning phase (Afshari et al., 2005). Because the living room door was opened during candle extinguishing, the number concentrations of particles $<0.025 \mu\text{m}$ in diameter showed a slight increase after half an hour in the kitchen. We also noticed that newly formed particles during candle burning do tend to grow over 50 nm in diameter; a finding was previously supported by Fine et al. (1999) that candle burning produces few vapor compounds that reduce their probability to grow by condensation.

Fan and Zhang (2001) reported that a significant amount of fine particles larger than $0.1 \mu\text{m}$ in diameter are produced during candle burning and oil lamp activities in a small chamber (0.15 m^3). The lower size in their measurement did not go below $0.1 \mu\text{m}$ in diameter; however, their results indicated a clear increase in the number concentrations of particles smaller than $0.3 \mu\text{m}$ in diameter. Possibly a soot mode as reported by Fine et al. (1999). Cole (1998) has also showed that soot particles from candles are small, ranging between 0.03 – $3 \mu\text{m}$, and it could stay airborne for a significant time period. Compared to our findings, we did not observe that soot mode, possibly, because our measurement was conducted in a room that is relatively bigger than the chambers used by Fan and Zhang (2001) and Fine et al. (1999).

4.4.3. Aroma lamp

Aroma lamp activities were performed three times in the living room (November 21, 22, and 24); the effect was clearly seen in one case only (Figs. 6b and 7c). The reason we did not observe the effect on November 21 and 22 was mainly because they occurred during cooking activities in the kitchen (Fig. 6c).

In general, the effect of aroma lamp can be interpreted as a combination between candle burning and the aroma oil evaporation (Fig. 7c,d). Two distinguished modes were observed with GMD 0.025 and $0.15 \mu\text{m}$ and number concentration of 500 cm^{-3} and 2000 cm^{-3} , respectively, (background concentration was about 1500 cm^{-3}). When the aroma lamp was extinguished, the number concentration of the second mode disappeared and the

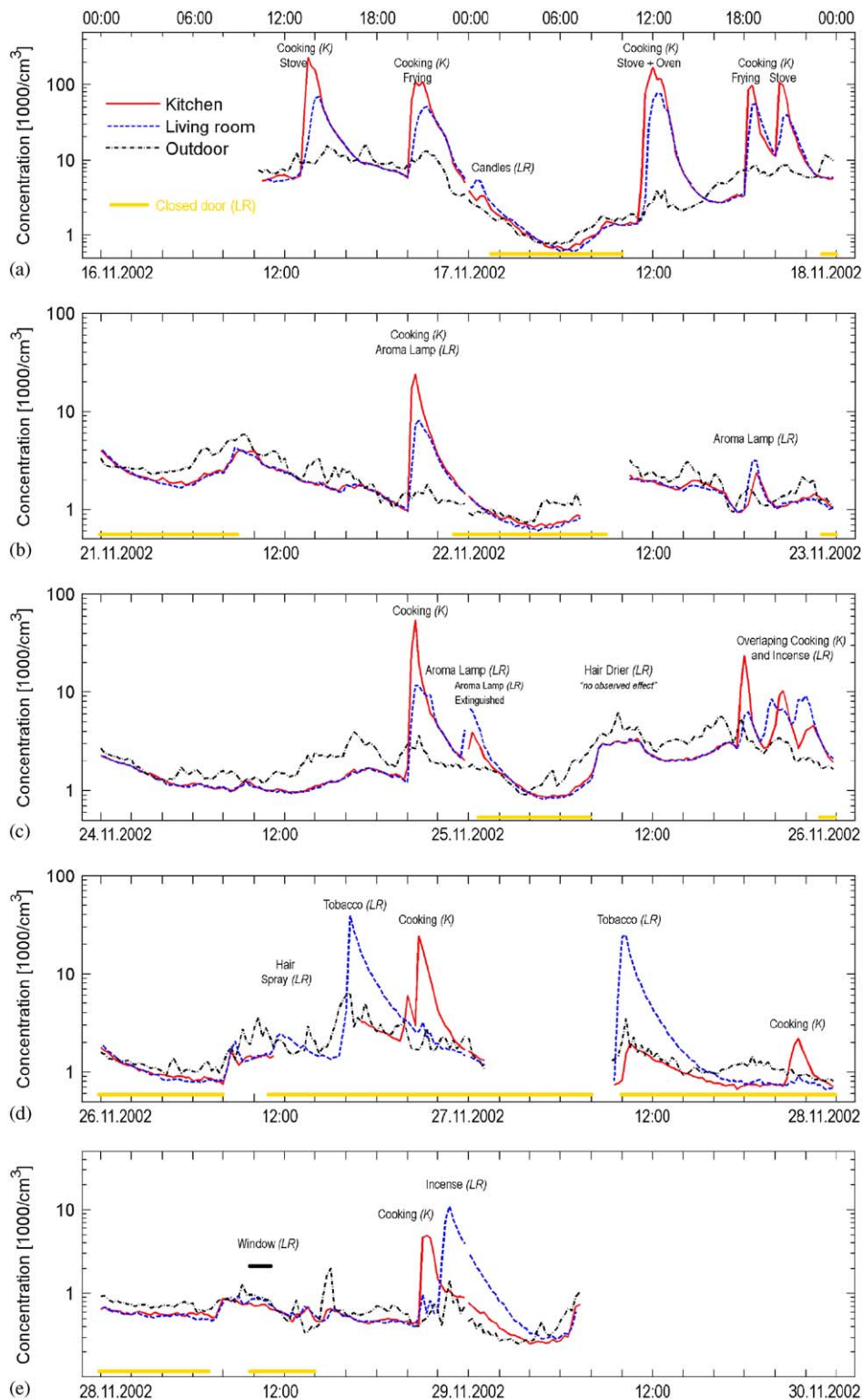


Fig. 6. Total particle number concentrations during different indoor activities. Each activity is indicated by its name and location as living room (LR) and kitchen (K).

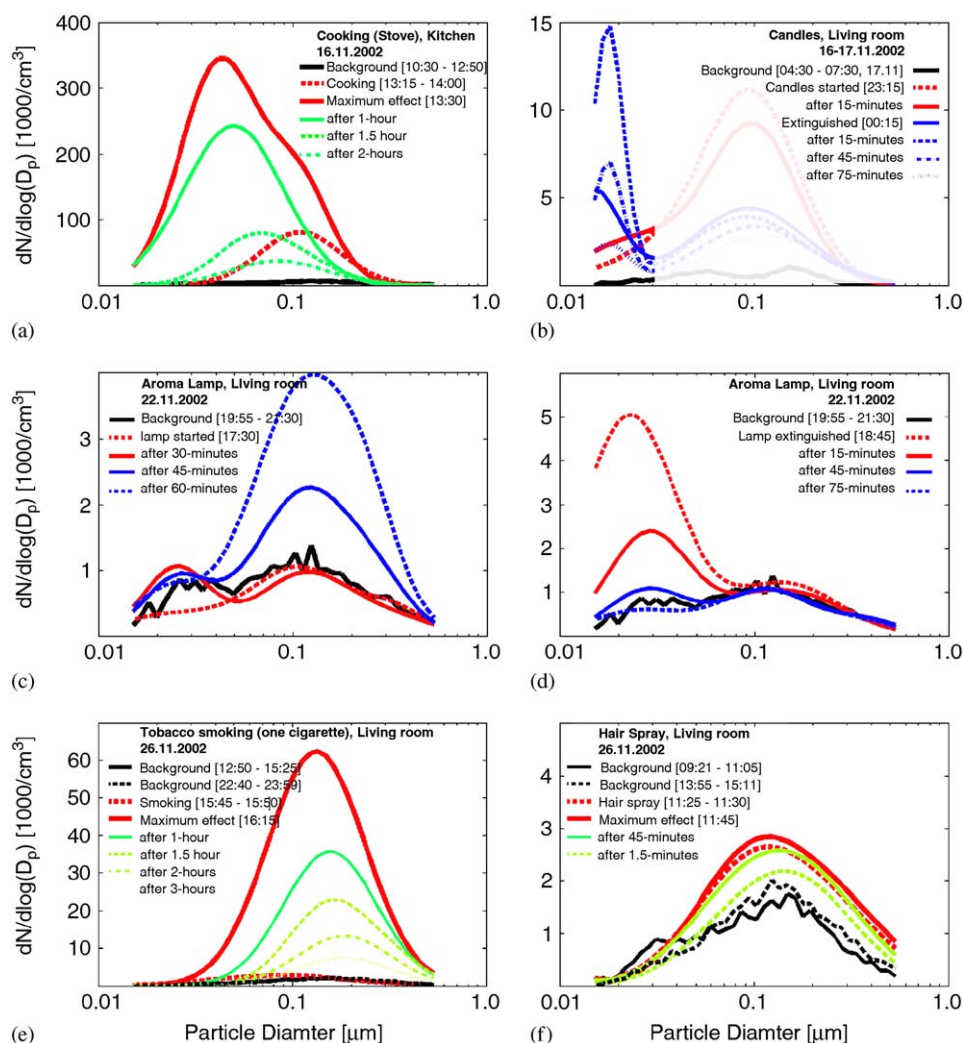


Fig. 7. Particle number size distributions from different indoor activities. Each activity is indicated by its name and location. Note that the measured particle number size distributions in the current study were based on their wet electrical-mobility diameters.

number concentration of the first mode increased by 2000 cm^{-3} (Fig. 7d).

4.4.4. Tobacco smoking

Smoking one cigarette in the living room increased the total particle number concentrations to $3.6 \times 10^4 \text{ cm}^{-3}$ over the base-line, which was around $6 \times 10^3 \text{ cm}^{-3}$. The effect of tobacco smoking was observed in particles $>0.03 \mu\text{m}$ in diameter (Figs. 6d and 7e). Even though the living room door was closed, the effect was also observed in the kitchen after one hour when the peak value of the total particle number concentration was 0.1 its value in the living room.

A fan was operating in the living room to improve the indoor air mixing during tobacco

smoking; however, the decay rate of the emitted aerosol particles was smaller than that for cooking aerosol particles (Fig. 6d). For example, the aerosol particles due to tobacco smoking stayed airborne for about 8–10 h. In general, tobacco smoke particles are assumed to be conservative; that is, they do not coagulate, evaporate, or grow by condensation (Miller and Nazaroff, 2001). Furthermore, the deposition rate of fine particles due to tobacco smoke is rather low (Xu et al., 1994).

He et al. (2004) measured the total particle number concentrations (down to 7 nm in diameter) during tobacco smoking; they reported comparable values (about $26,600 \text{ cm}^{-3}$, 1.54 the background value) to our results for the maximum number concentration. In their study, Morawska et al.

(2003) reported higher particle number concentrations (maximum value ranging between 2×10^5 and $3.5 \times 10^6 \text{ cm}^{-3}$) during tobacco smoking. However, it was not reported in both studies how many cigarettes were smoked and whether they were smoked simultaneously. Afshari et al. (2005) tested three cases of cigarette smoking during 10 min for each cigarette; the number concentration of fine particles and also particles larger than $1 \mu\text{m}$ suddenly increased right after smoking started. The maximum number concentration of UFP was about $2.13 \times 10^5 \text{ cm}^{-3}$ and they stayed airborne for about 20 min. The UFP number concentration decayed to the background level within 300 min. Afshari et al. (2005) also reported that the particle number concentrations of the fine fraction between $0.4\text{--}0.6 \mu\text{m}$ showed another maximum ($25\text{--}30 \text{ cm}^{-3}$) after 100 min of the smoking event.

4.4.5. Hair spray and hair drier

It was reported that the hair drier was used four times. Two of them were neglected because of invalid aerosol data and the other two did not indicate significant sources of aerosol particles that can be considered negligible (Fig. 6c). Similarly, He et al. (2004) presented that the ratio of the particle number concentration during hair drier activity to the background number concentration was about 1.06. However, they reported that the ratio for particulate mass, namely $\text{PM}_{2.5}$, concentration was about 1.36. This indicates that hair drier influences particles larger than $0.1 \mu\text{m}$ in diameter, which has the biggest fraction of the mass concentration.

Hair spray was reported twice; one was eliminated because of invalid aerosol data. The number concentrations of particles between 0.03 and $0.5 \mu\text{m}$ showed an increment of about 1000 cm^{-3} (Fig. 6d). It seems that aerosol particles produced from hair sprayer survive longer than tobacco smoke particles. Even though the number of emitted particles during 5-min of hair spray is lower than that produced during 5-min smoking, but this small amount of hair spray aerosols survived for about 4-h (Fig. 6d and 7f). Hair sprayer seems to have similar effect as that observed for air freshener sprayers. Afshari et al. (2005) have reported $3 \times 10^4 \text{ cm}^{-3}$ during air freshener spraying with a majority in the UFP size range in addition with a significant increase in the number concentration of coarse particles.

4.4.6. Incense sticks

The behavior of aerosol particles during incense sticks burning (November 28, 2002) showed similar modal structure as that observed for tobacco smoke particles; the decay pattern was also similar (Fig. 6e). The total particle number concentration suddenly increased from 8×10^2 to $1.2 \times 10^4 \text{ cm}^{-3}$ when the incense stick was started. Because the living room door was closed during incense stick burning, the effect was negligible in the kitchen.

Incense stick burning was also done on another two occasions (November 25, 2005) when cooking activities occurred in the kitchen. Therefore, the effect was difficult to be interpreted because of the overlap between cooking and incense activities on that specific day (Fig. 6c).

4.4.7. Open windows

As expected, an open window increases the penetration factor and enhance the ventilation rate. Once the living room window was opened the number concentration increased to a value close to that observed outdoors indicating penetration factor close to unity. In the meanwhile, the living room door was kept closed; therefore the particle number concentrations in the kitchen did not show any significant changes (Fig. 6e).

4.4.8. Penetration of indoor aerosols to the outdoor air

Even though the windows were kept closed most of the time, indoor aerosol particles produced during cooking, tobacco smoking, and incense stick burning were observed outdoors (Fig. 6). The main reason behind that is the house structure that was relatively old and it was leaking. However, the effect was smaller than what was observed indoors; possibly because a big fraction of the produced indoor aerosols were lost while penetrating outdoors and also due to substantial dilution by the outdoor air. Loss of indoor aerosols while transported outdoors is mainly due to deposition across the building shell while penetrating outdoors.

4.5. Emission rates: indoor aerosol model simulations

The main reason for the model simulations in the current study is to estimate the emission rates of aerosol particles during different indoor activities. We only investigated and simulated emission rates during some activities that occurred separately either in the kitchen or in the living room. In

general, model simulations in the current study were challenging because of the ventilation type (natural ventilation) that caused variable ventilation rate. In addition, the building shell was relatively old and it was leaking. Consequently, the penetration factor showed considerable changes that were probably due to the varying ambient weather conditions and the penetration path across the building shell (e.g. Chan, 2002). Furthermore, the air flow streams were unknown indoors and therefore the air exchange rates between indoor compartments were unknown.

To keep the simulations as simple as possible we assumed two indoor compartments: kitchen and living room (Fig. 8). After testing several model simulations we considered the part of the hallway that connected the kitchen and the living room as an air exchange path way; the evolution of aerosol particles was assumed negligible while exchanged between the living room and the kitchen via the hallway. We considered the remaining part of the hallway as non-interacting because assuming a separate compartment for that part did not improve the simulation accuracy. All other rooms were assumed non-interacting with the kitchen and the living room as described in Section 2.2. The model simulations were performed separately for each day; therefore, every day was a separate case. Two main periods were chosen for every day: Period-I when

the living room door was opened and Period-II when it was closed.

Following we summarize a step-by-step procedure to determine the emission rates of indoor aerosol particles. For that purpose we selected a time period of three successive days (November 17–19, 2002). Before estimating the emission rates, we first predicted the best-fit (optimal) values for the penetration factor, ventilation rate, and the friction velocity; i.e. deposition rate. Then the air exchange rate between the kitchen and the living room was predicted by investigating the transport of emitted indoor aerosols between the kitchen and the living room.

4.5.1. Scenario-I: penetration factor, ventilation rate, and deposition rate

To estimate the penetration factor, ventilation rates, and friction velocity (i.e. deposition rate) we initially assumed the kitchen and the living room are not interacting with each other and the number concentrations in every room is relatively the same; this assumption is valid based on the results and the related discussion presented in Fig. 2. We performed several simulations by using different curves for the penetration factor and different values for the ventilation rates and friction velocities. As a measure of the simulation quality in this scenario

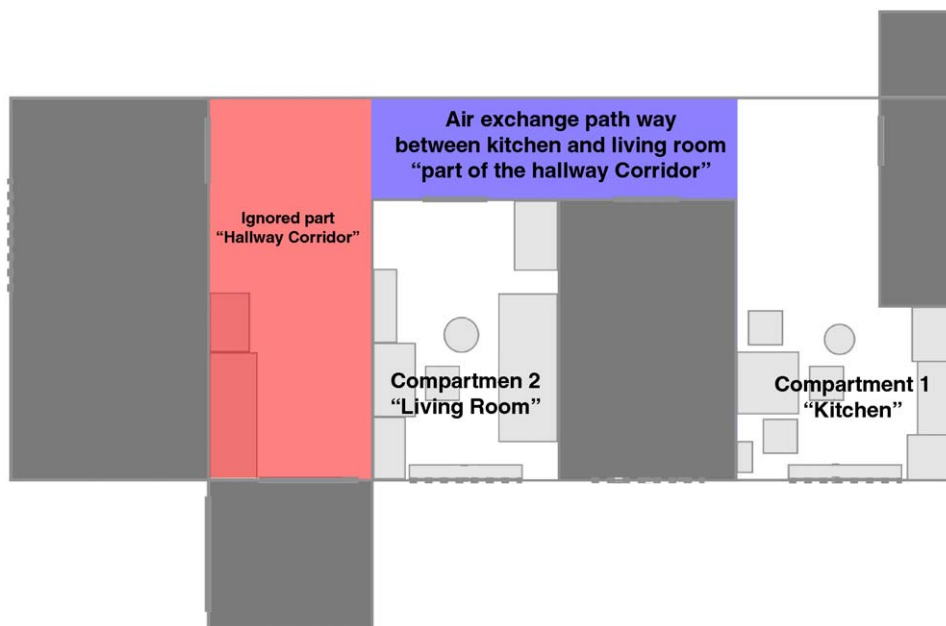


Fig. 8. Compartments to be considered in the model simulations. A part of the hallway was ignored and the remaining part of the hallway that connects the kitchen and the living room was considered as an air exchange path way.

we compared the simulated particle number concentrations with the measurement. Because the indoor activities took place during daytime, the comparison was restricted to the night time periods. We assumed that the ventilation conditions should not vary considerably during a day unless a window or a door was opened. Note that this assumption is not valid when the ambient conditions vary considerably.

Our initial guess for penetration factor, which is the most important parameter, was based on the *I/O* investigations. Fig. 9 presents a range of the best-fit penetration factor curve as a function of the particle diameter. As expected from the *I/O* analysis, the penetration factor was similar for the living room and the kitchen. As a general note, the penetration factor was greater during period-I than during period-II. Period-I was mainly during daytime and Period-II was mainly during nighttime. Zhu et al. (2005) also reported higher *I/O* ratios during daytime in a naturally ventilated house nearby a freeway.

We iterated the ventilation rates between 0.15 and 3.00 h⁻¹. If all the windows were closed, it is obvious that the ventilation rate does not vary significantly assuming the ambient conditions did not change dramatically. Therefore, the ventilation rates were assumed constant during a period of simulation. When all windows were closed the predicted ventilation rate varied between 0.6 and 1.2 h⁻¹ (measured value for the living room was about 0.39 ± 0.13 h⁻¹ with a variation during daytime between 0.27 and 0.61 h⁻¹) for both the kitchen and the living room. Our prediction for the

ventilation rate was in good agreement with the measurement.

The friction velocity was chosen based on the decay rate analysis of indoor aerosol particles. We iterated the friction velocity between 5 and 100 cm s⁻¹. We assumed that the friction velocity is rather constant as long as the ventilation rate is not varying and there is no enhanced air mixing in the indoor air. The predicted friction velocities ranged between 10 and 30 cm s⁻¹. As mentioned and discussed before, the friction velocity obtained from the model simulation is smaller than our previous guess presented in Fig. 5.

After investigating the indoor–outdoor relationship of aerosol particles during November 17 the simulation periods did not coincide with the living room door conditions. It seems that the kitchen window was opened during one cooking activity on November 17 and that was not reported.

4.5.2. Scenario-II: air exchange between the kitchen and the living room

So far we assumed the kitchen and the living room are not interacting with each others; i.e. the air exchange rate terms were set to zero. In this scenario we predicted the air exchange rate between the kitchen and the living room. Note that the predicted air exchange rate represents an effective value because we assumed a part of the hallway is a passive path way for the air exchange between the kitchen and the living room.

In the first place, we perform initial estimations for the emission rates in every compartment

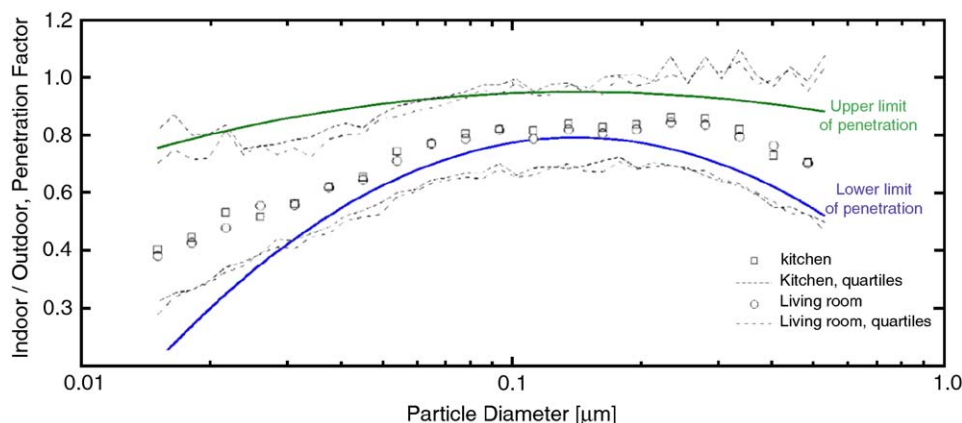


Fig. 9. A range of the optimal penetration factor curve used in the indoor aerosol model simulations. Note that the measured particle number size distributions in the current study were based on their wet electrical-mobility diameters.

(kitchen or living room) by assuming no air exchange between them. Note that we set the emission rate to zero in the living room during cooking activities and similarly we set the emission rate to zero in the kitchen during all other activities that took place in the living room. These emission rates were then fed back in the model simulation to predict the air exchange rate between the kitchen and the living room.

When predicting the air flow rate from the kitchen to the living room we focused on the cooking activities. During a cooking activity, the particle number concentrations were suddenly increased in the kitchen and after a while they were observed in the living room. The time-lag between the number concentrations peaks in the kitchen and in the living room as well as their absolute value were a good marker for the air flow rate from the kitchen to the living room. In that sense, we iterated the value of the air flow rate from the kitchen to the living room until we observed a good match between the simulation results and the measurement of the particle number concentrations.

Similarly, we predicted the air flow rate from the living room to the kitchen during candle burning, cigarette smoking, and incense sticks burning. According to this analysis, the air exchange rates between the kitchen and the living room varied between 0.0097 and $0.0150 \text{ m}^3 \text{ s}^{-1}$; the higher value was observed when the living room door was opened.

4.5.3. Scenario–III: final emission rates

In the previous scenario we could obtain initial estimates for the emission rates indoors. In fact, these emission rates are not final because they were estimated by assuming the kitchen and the living room are non-interacting. Assuming the optimal (best-fit) values for the input parameters to the MC-SIAM are an acceptable solution, we can proceed to fine tune the emission rates as described in Section 3.2. Nevertheless, the emission rate analysis also indicated the existence of un-identified indoor sources of aerosol particles.

In summary, Fig. 10 presents the simulation results of the particle number size distributions according to these Scenarios for the time period November 17–19, 2002. First of all, it should be clearly noticed that the emitted aerosol particles during cooking activities were also observed outdoors; as marked by C1–C5 (Fig. 10a–d). The

stronger the cooking activity was the more the aerosol particles were observed outdoors. Figs. 10e,f, illustrate the simulations by using the optimal parameters including the penetration factor, ventilation rate, friction velocity, and the air exchange rate between the kitchen and the living room. Compared to the measurement, there is a good agreement between the model simulation and the measurements for the nighttime periods (Figs. 10c–f).

The emission rates, in their final estimations, are presented in Figs. 10g–j. The particle emissions during candle burnings were $\sim 5 \text{ particles cm}^{-3} \text{ s}^{-1}$ in the living room and the emissions were relatively very small in the kitchen. In fact, the emissions during candle burnings should be zero in the kitchen. Afshari et al. (2005) reported that pure wax candles emitted about $190 \text{ particles cm}^{-3} \text{ s}^{-1}$ inside a test chamber with 32 m^3 volume whereas scented candles emitted about $45 \text{ particles cm}^{-3} \text{ s}^{-1}$.

Cooking, in general, produced aerosol particles with emission rates as high as $360 \text{ particles cm}^{-3} \text{ s}^{-1}$ ($6 \times 10^{11} \text{ particles min}^{-1}$), mainly UFP, assuming the air is well-mixed within the kitchen. However, to compensate for a good match between the simulation and the measurement, an emission rate as high as $10 \text{ particles cm}^{-3} \text{ s}^{-1}$ in the living room. Our estimation for the emission rates due to cooking activities agrees with previous studies by Afshari et al. (2005) and He et al. (2004) where they reported aerosol particles emissions 1.27×10^{11} – $8.27 \times 10^{11} \text{ particles min}^{-1}$ during different cooking activities including oven, frying, stove (electrical and gas), and toasting. They also indicated that frying and stove cooking can be the strongest sources.

We also estimated the emission rates of indoor aerosol particles during tobacco smoking ($\sim 36 \text{ particles cm}^{-3} \text{ s}^{-1} \leftrightarrow 0.84 \times 10^{11} \text{ particles min}^{-1}$) and incense stick burning ($\sim 10 \text{ particles cm}^{-3} \text{ s}^{-1} \leftrightarrow 0.23 \times 10^{11} \text{ particles min}^{-1}$). He et al. (2004) reported higher emission rates (about $1.91 \times 10^{11} \text{ particles min}^{-1}$) due to tobacco smoking. On the other hand, Afshari et al. (2005) showed that smoking cigarettes would emit aerosol particles with a rate around $3.76 \times 10^{11} \text{ particles min}^{-1}$. Based on the indoor model simulations and the emission rate analysis, aerosol particles produced during tobacco smoking and incense stick burning remain airborne for a longer time than cooking particles. It seems that tobacco smoke and incense burning particles are less reactive than cooking particles.

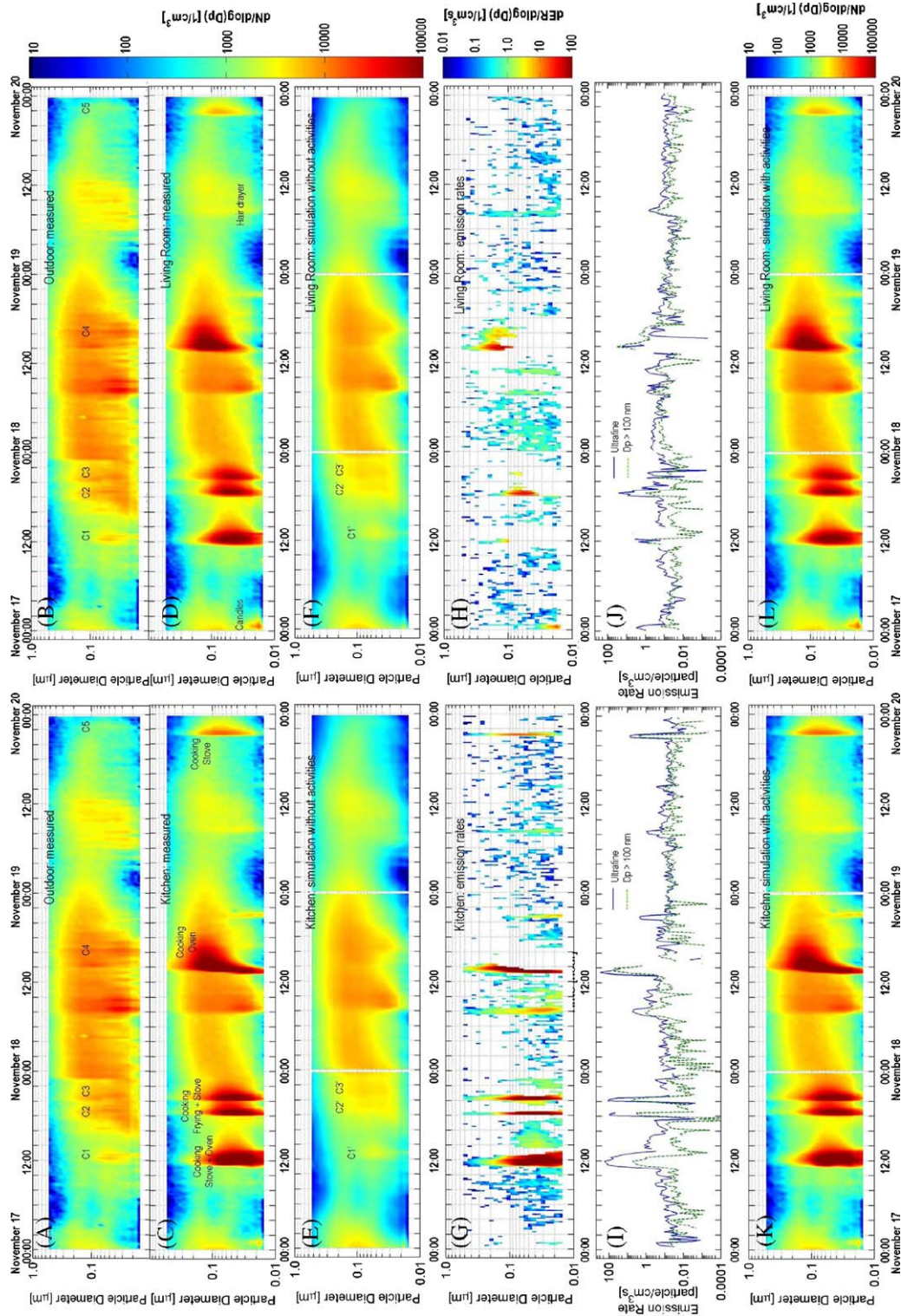


Fig. 10. Particle number size distribution spectra as measured (A,B) outdoors and indoors (C) in the kitchen and (D) in the living room. The indoor aerosol model simulation results according to Scenarios I and II in (E) the kitchen and (F) the living room by neglecting indoor activities and using the optimal values of the model input parameters. Size-specific emission rate spectra in (G) the kitchen and (H) the living room and those for ultrafine particles are, respectively, presented in (I,J). The indoor aerosol model simulation results by feeding back the final emission rates and the enhanced sink rates, as predicted with the MC-SIAM are, respectively, presented in (K,L). The indoor activities are indicated by their name and the corresponding marks C1–C5 indicate the penetrated indoor aerosol particles into the outdoor air after undergoing intensive cooking in the kitchen.

4.5.4. Scenario–IV: verifications of the optimal input parameters and the emission rates

To verify the model simulations results, we fed back the final emission rates into the indoor model simulation. As expected, the simulation results showed good agreement with the measurement and it reproduced the effects of indoor activities rather well (Figs. 10k,l). However, we noticed that after cooking activities there is a need for an enhanced sink (less than $10 \text{ particles cm}^{-3} \text{ s}^{-1}$) for a short period (few minutes) to match the model simulations with the measurement. Similarly, Afshari et al. (2005) also showed that varying sink rates for emitted UFP during different activities within a test chamber; the strongest sinks ($0.74\text{--}0.95 \text{ h}^{-1}$) accompanied indoor activities with relatively high temperature such as during frying meat, heater, and radiator. The sink value was between 0.43 and 0.65 h^{-1} during tobacco smoking and scented/wax candles.

Based on these finding in our study and also by Afshari et al. (2005), the varying sink value as well as the evolution of the emitted particles encourages the need of a more advanced indoor aerosol model to describe other physical–chemical processes that take place in the evolution of emitted indoor aerosol particles. In general, aerosol particles produced during cooking activities were, as expected, dependent on the type and way of cooking.

Finally, it should be mentioned that this kind of model simulations is very challenging and the decision made for these optimal parameters was performed with a great care based on our understanding to the indoor–outdoor relationship of aerosol particles. This set of input parameters is therefore one solution and it is not absolute; we believe there are many sets of parameters that lead to acceptable solutions for an indoor–outdoor aerosol problem. However, a good understanding to the indoor–outdoor aerosol problem and after investigating the indoor-to-outdoor relationship of aerosol particles would help in determining the most suitable set of parameters. In addition, further investigations on the fate of indoor aerosol particles help in determining the first guess of the friction velocity to be used in the deposition model that predicts the deposition velocity of aerosol particles on indoor surfaces.

5. Summary and conclusions

Characterization of indoor aerosol particles and their emission rates have been given increasing

attention during the recent years. However, few studies have presented quantitative determination of aerosol particle emissions from indoor sources. In the current study we presented and investigated: (1) the physical characteristics of indoor aerosol particles during different indoor activities, (2) estimate the emission rates of size-fractionated indoor aerosol particles during some of these activities, and (3) investigated the indoor-to-outdoor relationship of aerosol particles. We utilized a multi-compartment and size-resolved indoor aerosol model (MC-SIAM) to predict the emission rates of aerosol particles, penetration factor, deposition rate of aerosol particles, ventilation rate, and the air exchange between the kitchen and the living room.

As expected, the natural ventilation did not provide a reliable and controlled relationship (including penetration factor and ventilation rate) between the indoor and outdoor aerosol particles. When the windows and the main door were closed for a long period and there were minor indoor activities that did not produce significant amounts of aerosol particles, the particle number concentration showed similar levels in different indoor locations. It seems that a simple model is not able to describe the fate of indoor aerosols within a multi-compartment construction; instead, a numerical and dynamic model with a multi-compartment approach is needed. The predicted deposition rate was comparable to previous studies with friction velocity between 10 and 30 cm s^{-1} and surface area to volume ratio around $2.9\text{--}3.1 \text{ m}^{-1}$. The predicted penetration factor for the house was equivalent to G3 filter standards. The predicted ventilation rate varied between 0.6 and 1.2 h^{-1} .

As previous studies have shown, cooking and tobacco smoking are major sources of indoor aerosols; the total particle number concentration was, respectively, about 1.8×10^5 and $3.6 \times 10^4 \text{ cm}^{-3}$ with emission rates around 380 and $36 \text{ cm}^{-3} \text{ s}^{-1}$. Other activities including candle burning, aroma lamp, and hair spray were minor indoor sources in comparison to cooking and tobacco smoking. Incense stick burning was an intermediate source with emission rate below $10 \text{ cm}^{-3} \text{ s}^{-1}$. The effect of hair drier was negligible. Some indoor sources were observed from the data analysis even though they were not reported. During intensive cooking activities the outdoor aerosol particle concentrations were also affected even though windows were closed.

Based on the indoor model simulations and the emission rate analysis, aerosol particles produced during tobacco smoking and incense stick burning remain airborne for a longer time than cooking particles. It seems that aerosol particles emitted during tobacco smoking and incense stick burning undergo different processes; therefore, there is a need for a combined physical–chemical indoor aerosol model to better describe the evolution of indoor aerosol particles due to different activities.

In general, tobacco smoking indoors is very harmful (e.g. Lai, 2004; Miller and Nazaroff, 2001; Kleeman et al., 1999). Based on the current study, smoking one cigarette can produce aerosol particles equivalent to the amount produced during intermediate cooking for about half hour and tobacco smoke particles may stay airborne up to 10 h.

Indoor aerosol model simulations are very challenging especially when natural ventilation is used for a multi-compartment indoor environment. In general, an indoor–outdoor aerosol problem may have many solutions and thus different sets of model parameters. Therefore, a good understanding to the indoor–outdoor aerosol problem and preliminary investigations for the indoor-to-outdoor relationship of aerosol particles would help in determining the most suitable set of model parameters.

The current study presented a useful procedure to easily determine unknown ventilation rate, penetration factor, fate of indoor aerosol particles, and air exchange rate between indoor compartments. Our results are building specific and user influenced.

Acknowledgments

This work was supported by the GA CR under grant 101/04/1190. Funding from Academy of Finland and the TEKES (Finnish Funding Agency for Technology and Innovation) is acknowledged. The authors would like to thank Dr. Ladislav Moucka and Dipl. Ing. Ales Fronka from the National Radiation Protection Institute Prague for carrying out the air exchange measurements in the house.

References

Abt, E., Suh, H.H., Allen, G., Koutrakis, P., 2000a. Characterization of indoor particle sources: a study conducted in

the metropolitan Boston area. *Environmental Health Perspective* 108, 35–40.

Abt, E., Suh, H.H., Catalano, P., 2000b. Relative contribution of outdoor and indoor particle sources to indoor concentrations. *Environmental Science and Technology* 34, 3579–3587.

Afshari, A., Matson, U., Ekberg, L.E., 2005. Characterization of indoor sources of fine and ultrafine particles: a study conducted in a full-scale chamber. *Indoor Air* 15, 141–150.

Asmi, A.J., Pirjola, L.H., Kulmala, M., 2004. A sectional aerosol model for submicron particles in indoor air. *Scandinavian Journal of Work, Environment, and Health* 30 (Suppl. 2), 63–72.

Bagley, S.T., Baumgard, K.J., Gratz, L.D., Johnson, J.H., Leddy, D.G., 1996. Characterization of fuel and after treatment device effects on diesel emissions. Research Report Number 76, Health Effects Institute, Cambridge, MA.

Birmili, W., Wiedensohler, A., Heintzenberg, J., Lehmann, K., 2001. Atmospheric particle number size distribution in central Europe: statistical relations to air masses and meteorology. *Journal of Geophysical Research* 106 (D23), 32005–32018.

Borchellini, R., Fürbringer, J.-M., 1999. An evaluation exercise of a multizone air flow model. *Energy and Buildings* 30, 35–51.

Chan, A.T., 2002. Indoor–outdoor relationships of particulate matter and nitrogen oxides under different outdoor meteorological conditions. *Atmospheric Environment* 36, 1543–1551.

Chao, C.Y.H., Wan, M.P., Cheng, E.C.K., 2003. Penetration coefficient and deposition rate as a function of particle size in non-smoking naturally ventilated residences. *Atmospheric Environment* 37, 4233–4241.

Cole, C., 1998. Candle Soot Deposition and Its Impacts on Restorers. Sentry Construction Company, USA.

Dennekamp, M., Howarth, S., Dick, C.A.J., Cherrie, J.W., Donaldson, K., Seaton, A., 2001. Ultrafine particles and nitrogen oxides generated by gas and electric cooking. *Occupational and Environmental Medicine* 58, 511–516.

Fan, C.W., Zhang, J.J., 2001. Characterization of emissions from portable household combustion devices: particle size distributions, emission rates and factors, and potential exposures. *Atmospheric Environment* 35, 1281–1290.

Feustel, H.E., 1999. COMIS—an international multizone air-flow and contaminant transport model. *Energy and Buildings* 30, 3–18.

Fine, P.M., Cass, G.R., Simoneit, B.R.T., 1999. Characterization of fine particle emissions from burning church candles. *Environmental Science and Technology* 33, 2352–2362.

Flückiger, B., Seifert, M., Koller, T., Monn, C., 2000. Air quality measurements in a model kitchen using gas and electric stoves. *Proceedings of Healthy Buildings*, vol. 1, pp. 567–572.

Friess, H., Yadigaroglu, G., 2002. Modeling of the resuspension of particle clusters from multilayer aerosol deposits with variable porosity. *Journal of Aerosol Science* 33, 883–906.

Gadgil, A.J., Lobscheid, C., Abadie, M.O., Finlayson, E.U., 2003. Indoor pollutant mixing time in an isothermal closed room: an investigation using CFD. *Atmospheric Environment* 37, 5577–5586.

Haas, A., Weber, A., Dorer, V., Keilholz, W., Pelletret, R., 2002. COMIS v3.1 simulation environment for multizone air flow and pollutant transport modelling. *Energy and Buildings* 34, 873–882.

He, C., Morawska, L., Hitchins, J., Gilbert, D., 2004. Contribution from indoor sources to particle number and mass

- concentrations in residential houses. *Atmospheric Environment* 38, 3405–3415.
- Helsper, C., Moltr, W., Löffler, F., Wadenpohl, C., Kaufmann, S., Wenninger, G., 1993. Investigation of a non-aerosol generator for the production of carbon aggregate particles. *Atmospheric Environment* 27A, 1271–1279.
- Hinds, W.C., 1999. *Aerosol Technology*, second ed. Wiley, New York.
- Hussein, T., Hämeri, K., Aalto, P., Asmi, A., Kakko, L., Kulmala, M., 2004a. Particle size characterization and the indoor-to-outdoor relationship of atmospheric aerosols in Helsinki. *Scandinavian Journal of Work, Health and Environment* (Suppl. 2), 54–62.
- Hussein, T., Puustinen, A., Aalto, P.P., Mäkelä, J.M., Hämeri, K., Kulmala, M., 2004b. Urban aerosol number size distributions. *Atmospheric Chemistry and Physics* 4, 391–411.
- Hussein, T., Dal Maso, M., Petäjä, T., Koponen, I.K., Paatero, P., Aalto, P.P., Hämeri, K., Kulmala, M., 2005a. Evaluation of an automatic algorithm for fitting the particle number size distributions. *Boreal Environment Research* 10, 337–355.
- Hussein, T., Hämeri, K., Aalto, P.P., Kulmala, M., 2005b. Modal structure and spatial-temporal variations of urban and suburban aerosols in Helsinki area. *Atmospheric Environment* 39, 1655–1668.
- Hussein, T., Hämeri, K., Heikkinen, M.S.A., Kulmala, M., 2005c. Indoor and outdoor particle size characterization at a family house in Espoo—Finland. *Atmospheric Environment* 39, 3697–3709.
- Hussein, T., Korhonen, H., Herrmann, E., Hämeri, K., Lehtinen, K., Kulmala, M., 2005d. A multi-compartment and size-resolved indoor aerosol model. *Aerosol Science and Technology* 39, 1111–1127.
- Jamriska, M., Thomas, S., Morawska, L., Clark, B.A., 1999. Relation between indoor and outdoor exposure to fine particles near a busy arterial road. *Indoor Air* 9, 75–84.
- Jamriska, M., Morawska, L., Ensor, D.S., 2003. Control strategies for sub-micrometer particles indoors: model study of air filtration and ventilation. *Indoor Air* 13, 96–105.
- Jones, A.P., 1999. Indoor air quality and health. *Atmospheric Environment* 33, 4535–4564.
- Kleeman, M.J., Schauer, J.J., Cass, C.R., 1999. Size and composition distribution of fine particulate matter emitted from wood burning, meat charbroiling, and cigarettes. *Environmental Science and Technology* 33, 3516–3523.
- Klepeis, N.E., 1999. Validity of the uniform mixing assumption: determining human exposure to environmental tobacco smoke. *Environmental Health Perspectives* 107 (Suppl. 2), S357–S363.
- Korhonen, H., Lehtinen, K.E.J., Kulmala, M., 2004. Aerosol dynamic model UHMA: model development and validation. *Atmospheric Chemistry and Physics* 4, 757–771.
- Kousa, A., Kukkonen, J., Karppinen, A., Aarnio, P., Koskentalo, T., 2002. A model for evaluating the population exposure to ambient air pollution in an urban area. *Atmospheric Environment* 36, 2109–2119.
- Kulmala, M., Asmi, A., Pirjola, L., 1999. Indoor air aerosol model: the effect of outdoor air, filtration and ventilation on indoor concentrations. *Atmospheric Environment* 33, 2133–2144.
- Lai, A.C.K., 2004. Modeling of airborne particle exposure and effectiveness of engineering control strategies. *Building and Environment* 39, 599–610.
- Lai, A.C.K., Nazaroff, W.W., 2000. Modeling indoor particle deposition from turbulent flow onto smooth surfaces. *Journal of Aerosol Science* 31, 463–476.
- Lazaridis, M., Drossinos, Y., 1998. Multilayer resuspension of small identical particles by turbulent flow. *Aerosol Science and Technology* 28 (6), 548–560.
- LHEA: London Health Education Authority, 1997. *What People Think About Air Pollution, Their Health in General, and Asthma in Particular*. Health Education Authority, London.
- Lioy, P.J., Wainman, T., Zhang, J.J., 1999. Typical household vacuum cleaners: the collection efficiency and emissions characteristics for fine particles. *Journal of Air Waste Management Association* 49, 200–206.
- Long, C.M., Suh, H.H., Catalano, P.J., Koutrakis, P., 2001. Using time- and size-resolved particulate data to quantify indoor penetration and deposition behavior. *Environmental Science and Technology* 35, 2089–2099.
- Luoma, M., Batterman, S.A., 2001. Characterization of particulate emissions from occupant activities in offices. *Indoor Air* 11, 35–48.
- Mäkelä, J.M., Koponen, I.K., Aalto, P., Kulmala, M., 2000. One-year data of submicron size modes of tropospheric background aerosols in southern Finland. *Journal of Aerosol Science* 31, 596–611.
- Miller, S.L., Nazaroff, W.W., 2001. Environmental tobacco smoke particles in multizone indoor environments. *Atmospheric Environment* 35, 2053–2067.
- Morawska, L., Thomas, S., Jamriska, M., Johnson, G., 1999. The modality of particle size distributions of environmental aerosols. *Atmospheric Environment* 33, 4401–4411.
- Morawska, L., He, C., Hitchins, J., Gilbert, D., Parappukkaran, S., 2001. The relationship between indoor and outdoor airborne particles in the residential environment. *Atmospheric Environment* 35, 3463–3473.
- Morawska, L., He, C., Hitchins, J., Mengersen, K., Gilbert, D., 2003. Characteristics of particle number and mass concentrations in residential houses in Brisbane, Australia. *Atmospheric Environment* 37, 4195–4203.
- Mosley, R.B., Greenwell, D.J., Sparks, L.E., Guom, Z., Tucker, W.G., Fortmann, R., Whitfeld, C., 2001. Penetration of ambient fine particles into the indoor environment. *Aerosol Science and Technology* 34, 127–136.
- Nazaroff, W.W., Cass, G.R., 1986. Mathematical modeling of chemically reactive gases in indoor air. *Environmental Science and Technology* 20, 924–934.
- Nazaroff, W.W., Cass, G.R., 1989. Mathematical modeling of indoor aerosol dynamics. *Environmental Science and Technology* 23, 157–166.
- Nazaroff, W.W., Hung, W.-Y., Sasse, A.G.B.M., Gadgil, A.J., 1993. Predicting regional lung deposition of environmental tobacco smoke particles. *Aerosol Science and Technology* 19, 243–254.
- Offermann, F.J., Sextro, R.G., Fisk, W.J., Grimsrud, D.T., Nazaroff, W.W., Nero, A.V., Revzan, K.L., Yater, J., 1985. Control of respirable particles in indoor air with portable air cleaners. *Atmospheric Environment* 19, 1761–1771.
- Ott, W., Langan, L., Switzer, P., 1992. A time series model for cigarette smoking activity patterns: model validation for carbon monoxide and respirable particles in a chamber and an automobile. *Journal of Exposure Analysis and Environmental Epidemiology* 2 (Suppl. 2), S175–S200.
- Ott, W., Switzer, P., Robinson, J., 1996. Particle concentrations inside a tavern before and after prohibition of smoking:

- evaluating the performance of an indoor air quality model. *Journal of the Air and Waste Management Association* 46, 1120–1134.
- Pope, C.A., Dockery, D.W., 1999. Epidemiology of particle effects. In: Holgate, S.T., Samet, J.M., Koren, H.S., Maynard, R.L. (Eds.), *Air Pollution and Health*. Academic Press, San Diego, CA.
- Randerath, K., Putman, K.L., Mauderly, J.L., Williams, P.L., Randerath, E., 1995. Pulmonary toxicity of inhaled diesel exhaust and carbon black in chronically exposed rats. Part II: DNA damage. Research Report Number 68, Health Effects Institute, Cambridge, MA.
- Raunemaa, T., Kulmala, M., Saari, H., Olin, M., Kulmala, M.H., 1989. Indoor air aerosol model: transport indoors and deposition of fine and coarse particles. *Aerosol Science and Technology* 11, 11–25.
- Repace, J.L., Lowrey, A.H., 1980. Indoor air pollution, tobacco smoke, and public health. *Science* 208, 464–472.
- Riley, W.J., Mckone, T.E., Lai, A.C.K., Nazaroff, W.W., 2002. Indoor particulate matter of outdoor origin: importance of size-dependent removal mechanisms. *Environmental Science and Technology* 36, 200–207.
- Robinson, J., Nelson, W.C., 1995. National Human Activity Pattern Survey Data Base. United States Environmental Protection Agency, Research Triangle Park, NC.
- Schauer, J.J., Kleeman, M.J., Cass, G.R., Simoneit, B.R.T., 1999. Measurement of emissions from air pollution sources. I. C₁ through C₂₉ organic compounds from meat charbroiling. *Environmental Science and Technology* 33, 1566–1577.
- Schneider, T., Kildeso, J., Breum, N., 1998. A two compartment model for determining the contribution of sources, surface deposition and resuspension to air and surface dust concentration levels in occupied rooms. *Building and Environment* 34, 583–595.
- Shimada, M., Okuyama, K., Okazaki, S., Asai, T., Matsukura, M., Ishizu, Y., 1996. Numerical simulation and experiment on the transport of fine particles in a ventilated room. *Aerosol Science and Technology* 25, 242–255.
- Siegmann, K., Sattler, K., 1996. Aerosol from hot cooking oil, a possible health hazard. *Journal of Aerosol Science* 27, 493–494.
- Smolik, J., Lazaridis, M., Moravec, P., Schwarz, J., Zaripov, S.K., Ždimal, V., 2005. Indoor aerosol particle deposition in an empty office. *Water, Air, and Soil Pollution* 165, 301–312.
- Sohn, M.D., Lai, A., Smith, B.V., Sextro, R.G., Feustel, H.E., Nazaroff, W.W., 1999. Modeling aerosol behavior in multi-zone indoor environments. *Proceedings of Indoor Air'99*, Edinburgh, vol. 4, pp. 785–790.
- Thatcher, T.L., Layton, D.W., 1995. Deposition, resuspension, and penetration of particles within a residence. *Atmospheric Environment* 29, 1487–1497.
- Thatcher, T.L., Lai, A.C.K., Moreno-Jackson, R., Sextro, R.G., Nazaroff, W.W., 2002. Effects of room furnishings and air speed on particle deposition rates indoors. *Atmospheric Environment* 36, 1811–1819.
- Theerachaisupakij, W., Matsusaka, S., Akashi, Y., Masuda, H., 2003. Reentrainment of deposited particles by drag and aerosol collision. *Journal of Aerosol Science* 34, 261–274.
- Thornburg, J., Ensor, D.S., Rodos, C.E., Lawless, P.A., Sparks, L.E., Mosley, R.B., 2001. Penetration of particles into buildings and associated physical factors. Part I: model development and computer simulations. *Aerosol Science and Technology* 34, 284–296.
- Wallace, L., 2000. Real-time monitoring of particles, PAH, and CO in an occupied townhouse. *Applied Occupational and Environmental Hygiene* 15, 39–47.
- Whitby, K.H., 1978. The physical characteristics of sulfur aerosols. *Atmospheric Environment* 12, 135–159.
- Xu, M., Nematollahi, M., Sextro, R.G., Gadgil, A.J., Nazaroff, W.W., 1994. Deposition of tobacco smoke particles in a low ventilation room. *Aerosol Science and Technology* 20, 194–206.
- Zhu, Y., Hinds, W.C., Krudysz, M., Kuhn, T., Froines, J., Sioutas, C., 2005. Penetration of freeway ultrafine particles into indoor environments. *Journal of Aerosol Science* 36, 303–322.